# NATIONAL ADVISORY COMMITTEE FOR AERONAUTICS

## TECHNICAL NOTE 3158

## A SUBSTITUTE-STRINGER APPROACH FOR INCLUDING

## SHEAR-LAG EFFECTS IN BOX-BEAM VIBRATIONS

By William W. Davenport and Edwin T. Kruszewski

Langley Aeronautical Laboratory
Langley Field, Va.

NACA

Washington

January 1954

LE

A SUBSTITUTE-STRINGER APPROACH FOR INCLUDING

SHEAR-LAG EFFECTS IN BOX-BEAM VIBRATIONS

By William W. Davenport and Edwin T. Kruszewski

## SUMMARY

The use of the substitute-stringer approach for including shear lag in the calculation of transverse modes and frequencies of box beams is discussed. Various thin-walled hollow rectangular beams of uniform wall thickness are idealized by means of the substitute-stringer approach and the resulting frequencies of the idealized structures are compared with those of the original beams. The results indicate how the substitute-stringer idealization could be made in order to yield accurate representation of the shear-lag effect in dynamic analysis.

## INTRODUCTION

In determining analytically the natural transverse modes and frequencies of box beams, the influence of shear-lag effects may be of considerable importance, as indicated by investigations such as those presented in references 1 and 2. An appealing solution to the problem of including shear-lag effects in a dynamic analysis of a built-up box beam such as that shown in figure 1(a) would be to idealize the box beam into a simpler structure which involves fewer components but has essentially the same shear-lag properties. The simplest such idealized structure is the well-known substitute-stringer structure.

The substitute-stringer idealization is used by Kuhn and Peterson (ref. 3) in static problems for obtaining the maximum stresses of shell structures. There is, however, no indication that the idealized structures which have been defined for static problems would be effective in determining natural modes and frequencies. It is true that Anderson and Houbolt used the substitute-stringer idealization (ref. 2) to account for shear-lag effects on the natural bending frequencies of box beams. Their primary purpose, however, was to demonstrate the magnitude of the shear-lag effects; no investigation of the accuracy of the approach was presented.

The purpose of the present investigation is to indicate how the substitute-stringer idealization can be made (or, more precisely, where to locate the substitute stringers) in order that the dynamic behavior of the prototype and of the idealized structure will be essentially the same. This purpose is achieved by comparing the bending frequencies of several thin-walled rectangular tubes (which are analyzed exactly in ref. 1) with the frequencies obtained by an exact analysis of their idealized structures.

In this paper, the idealization of an actual box beam into its substitute-stringer structure is discussed. The aforementioned comparisons are then made and conclusions are drawn with regard to the accuracy of the procedure. A list of symbols is contained in appendix A and a vibration analysis of the substitute-stringer structure is included in appendix B. A pertinent extension of the solution of reference 1 is made in appendix C.

## THE SUBSTITUTE-STRINGER IDEALIZATION

A box beam which is typical of aircraft construction and its substitute-stringer structure are shown in figure 1. The idealized structure consists of four flanges and four stringers which carry only normal stress connected by sheets which carry only shear. The cross-sectional areas of the flanges and stringers of the idealized structure are determined so that their moments of inertia are the same as the moments of inertia of the spars and covers, respectively, of the original structure; the moments of inertia in each case are taken about the horizontal axis of symmetry. The over-all dimensions and the web and cover-sheet thicknesses are the same for both structures. The chordwise location of the substitute stringers, given by $b_S$, is, however, as yet unspecified; the value of $b_S$ determines the magnitude of the shear-lag effect in the idealized structure and is the quantity of paramount interest in this paper. Hereinafter, attention is directed to the effect on the vibration frequencies of varying $b_S$ and to the selection of the value of $b_S$ which yields accurate results.

## LOCATION OF THE SUBSTITUTE STRINGERS

In this section, comparisons are made between the frequencies of various thin-walled rectangular tubes such as that shown in figure 2 and the frequencies of their corresponding idealized structures. In each case the value of $b_S$ is permitted to vary between 0 and b. The frequencies of the rectangular tubes are obtained from a modification of

the exact series solution in reference 1; the frequencies for their ide-
alized structures are obtained from the solution presented in appendix B.
The exact series solution of reference 1 is modified to include only the
secondary effects considered in the substitute-stringer solution of appen-
dix B, that is, shear lag and transverse shear deformation.

The web and cover-sheet thicknesses and the cross-sectional areas
of the flanges and stringers of the idealized structure are obtained as
outlined in the preceding section and are (see figs. 1(b) and 2):

$$t_W = t_C = t$$

$$A_F = \frac{1}{3} at$$

$$A_L = bt$$

In order to preserve the inertial properties, the mass per unit length
of the substitute-stringer structure is taken equal to that of the rec-
tangular tube.

The effect of varying $b_S$ on the frequencies of the first three
symmetrical free-free modes of the idealized structure is shown graph-
ically in figures 3 to 6. In each case, the frequency $\omega$ is expressed
in the form of its relative error $\frac{\omega}{\omega_e} - 1$ when compared with the exact

frequency $\omega_e$ of the rectangular tube, and $b_S$ is expressed in the form
of the ratio $b_S/b_C$, wherein $b_C$ is the distance from the web to the
centroid of area of the half-cover. This ratio $b_S/b_C$ is used to accord
with past practice in static shear-lag investigations and also in the hope
that the results will be applicable to more general types of box beams.
It should be noted that, for the rectangular tubes, $b_C$ equals $b/2$.

The first case considered is that of a rectangular tube with a
cross-sectional aspect ratio $b/a$ of 3.6 and a plan-form aspect ratio
$L/b$ of 6.0. The curves of figure 3 cross the line of zero error at dif-
ferent values of $b_S/b_C$; thus no single value of $b_S/b_C$ gives exact fre-
quencies for all the modes. It is possible, however, to choose an "opti-
mum" value which gives nearly exact results for all the modes considered.
This optimum value, which has arbitrarily been selected so that the maxi-
mum of the errors in the frequencies of the first three modes is a mini-
mum, is $b_S/b_C = 0.56$. The maximum error in the frequencies for this
value is less than 1 percent.

The effects of different cross-sectional and plan-form aspect ratios are indicated in figures 4 and 5. In figure 4, results are shown for cross-sectional aspect ratios of 1 and ∞ (a limiting case) with a plan-form aspect ratio of 6.0. In figure 5, results are shown for plan-form aspect ratios of 2.0 and 12.0 with a cross-sectional aspect ratio of 3.6. The curves in figures 4 and 5 are similar in character to those presented in figure 3; they differ only in steepness and in the values of $b_S/b_C$ where the zero crossings occur. The optimum value of $b_S/b_C$ and the maximum percentage error of this value for each case are included in table 1. For all these cases, the maximum percentage errors are very small. It should be noted that, except for the case in which $b/a = 1.0$ and $L/b = 6.0$ and that in which $b/a = 3.6$ and $L/b = 2.0$, the optimum values of $b_S/b_C$ fall within a small range. In the first of these two cases, the shear-lag effect is very small in magnitude (see fig. 4); the second case is an extreme configuration, having a plan-form aspect ratio of 2.0. The results indicate, therefore, that for reasonable configurations with appreciable shear-lag effect, the optimum value of $b_S/b_C$ is relatively independent of the cross-sectional and plan-form aspect ratios.

The rectangular tubes treated thus far are admittedly not very realistic, and the extensibility of the results obtained to more usual box beams, such as that shown in figure 1(a), is questionable. For this reason, a generalization of the rectangular tube which more nearly represents actual structures has been considered. This generalized rectangular tube is assumed to have at each point of its cross section a thickness $t$ that carries shear and also a different thickness $t'$ that carries normal stress; this assumption approximates the situation in an actual structure in which flanges and stringers carry normal stress but do not carry shear. The exact series solution of reference 1 can be extended to this "dual-thickness" structure by the modification of the parameters shown in appendix C.

A particular example of this type of structure is considered in figure 6, where $L/b = 6.0$, $b/a = 3.6$, and $t'/t = 2.0$. Once again the maximum error for the optimum value of $b_S/b_C$ is small (see table 1). The optimum value of $b_S/b_C$ is less than the value obtained for the single-thickness counterpart; this reduction indicates a possible dependence of the optimum value of $b_S/b_C$ on the magnitude of the additional stress-carrying area of an actual structure.

## EVALUATION OF RESULTS

The ratios used for the configurations presented herein bracket those which would occur in most actual box beams. Cross-sectional and plan-form aspect ratios have been varied from 1 to ∞ and from 2 to 12, respectively. The ratio $t'/t$, which is a measure of the ratio of normal-stress-carrying area to shear-carrying area in the cover, has been varied from 1 to 2; representative values of $t'/t$ for actual box beams are within this range. The results in table 1 indicate that although these wide ranges of ratios were used, the optimum value of $b_S/b_C$ falls within a relatively narrow range. This result suggests the possibility that, in the absence of a more detailed investigation, a universal value of $b_S/b_C$ could be used. In order to demonstrate the validity of this conclusion, the values of the maximum of the errors in the first three vibration frequencies for a value of $b_S/b_C = 1/2$ are also presented in table 1. The errors exceed 2 percent only in the extreme cases.

Langley Aeronautical Laboratory,
     National Advisory Committee for Aeronautics,
          Langley Field, Va., November 2, 1953.

APPENDIX A

SYMBOLS


$A_F$            cross-sectional area of flange of substitute-stringer
                structure

$A_L$            cross-sectional area of substitute stringer

$A_S$            effective shear-carrying area

$A_S{}'$         parameter defined by equation (C7)

$A_T = A_F + A_L$

a               half-depth of beam

b               half-width of beam

$b_S$            distance between web and adjacent substitute stringer

$b_C$            distance between web and centroid of area of half-cover

C               constant

E               modulus of elasticity

G               shear modulus of elasticity (taken equal to $E/2.65$ in
                present paper)

I               bending moment of inertia

K               shear-lag parameter, $\sqrt{\dfrac{Gt_C}{Eb_S}\dfrac{A_T}{A_F A_L}}$

K'              parameter defined by equation (C5)

$k_B$            frequency coefficient, $\omega\sqrt{\dfrac{\mu L^4}{EI}}$

$k_S$            coefficient of shear rigidity, $\dfrac{1}{L}\sqrt{\dfrac{EI}{GA_S}}$

| | |
|---|---|
| $L$ | half-length of free-free beam |
| $N_n$ | parameter defined by equation (B22) |
| $N_n{}'$ | parameter defined by equation (C4) |
| $P_n$ | parameter defined by equation (B23) |
| $p$ | perimeter of cross section of beam |
| $s$ | distance along periphery of cross section of beam |
| $t$ | wall thickness of beam with uniform wall thickness; effective shear thickness for dual-thickness beam |
| $t_C$ | cover-sheet thickness |
| $t_W$ | web thickness |
| $t'$ | effective thickness for normal stress for dual-thickness beam |
| $T$ | maximum kinetic energy |
| $U$ | maximum strain energy |
| $u(x,s)$ | longitudinal displacement of a point on beam |
| $u_F$ | longitudinal displacement of point of flange in substitute-stringer structure |
| $u_L$ | longitudinal displacement of point of substitute stringer |
| $w$ | vertical displacement of cross section of beam |
| $x$ | longitudinal coordinate |
| $a_n, b_n, c_n$ | Fourier series coefficients |
| $i, n$ | integers |
| $\alpha_1, \alpha_2$ $\beta_1, \beta_2$ | parameters defined by equations (B26), (B27), (B29), and (B30) |

$\theta$           inclination of normal to the wall with the vertical

$\mu$           mass of beam per unit length

$\omega$           natural frequency of beam obtained by use of substitute-stringer approach

$\omega_e$           natural frequency of beam obtained by use of exact solution of reference 1

$\sigma_F$           longitudinal stress in flange of substitute-stringer structure

$\sigma_L$           longitudinal stress in substitute stringer

$\tau_C$           shear stress in cover sheet of substitute-stringer structure

$\tau_W$           shear stress in web of substitute-stringer structure

## APPENDIX B

### VIBRATION SOLUTION OF A FREE-FREE

### SUBSTITUTE-STRINGER STRUCTURE

The natural modes and frequencies of the substitute structure may be obtained by the method employed in reference 1, that is, the Rayleigh-Ritz energy procedure in conjunction with appropriate Fourier series expressions.

Let  $x$  be the longitudinal coordinate with its origin at the mid-point of the beam; then, by Hooke's law and the assumptions concerning the stress-carrying properties of the components of the structure given in the body of the paper, along with the assumption that cross sections maintain their shapes, the longitudinal stresses are

$$\sigma_F = E \frac{du_F}{dx} \tag{B1}$$

$$\sigma_L = E \frac{du_L}{dx} \tag{B2}$$

and the shearing stresses are

$$\tau_C = G \frac{u_F - u_L}{b_S} \tag{B3}$$

$$\tau_W = G\left(\frac{dw}{dx} - \frac{u_F}{a}\right) \tag{B4}$$

where  $u_F$  is the longitudinal displacement of a point on a flange,  $u_L$  is the longitudinal displacement of a point on a stringer, and  $w$  is the vertical displacement of a cross section of the beam.

From these expressions for the stresses, the maximum strain energy of the structure is

$$U = 2 \int_{-L}^{L} \left[ E\left(\frac{du_F}{dx}\right)^2 A_F + E\left(\frac{du_L}{dx}\right)^2 A_L + G\left(\frac{u_F - u_L}{b_S}\right)^2 t_C b_S + G\left(\frac{dw}{dx} - \frac{u_F}{a}\right)^2 t_W a \right] dx$$

$$\tag{B5}$$

and the maximum kinetic energy is

$$T = \frac{1}{2}\int_{-L}^{L} \mu\omega^2 w^2 \, dx \qquad (B6)$$

where $u_F$, $u_L$, and $w$ are now considered as the amplitudes of displacement for the particular mode considered, $\omega$ is the natural frequency of the mode, and $\mu$ is the mass per unit length of the structure which the substitute structure represents.

A natural mode of vibration must satisfy the variational equation

$$\delta(U - T) = 0 \qquad (B7)$$

where the variation is taken independently with respect to $u_F$, $u_L$, and w. Application of this principle to expressions (B5) and (B6) would result in the differential equations and the natural boundary conditions of the vibrational problem under consideration. However, Fourier series expressions for $u_F$, $u_L$, and w are used in conjunction with the variational procedure, rather than a direct attack on the differential equations and the boundary conditions.

Appropriate assumptions for the displacements for the symmetrical modes of a free-free beam are

$$w = C + \sum_{n=1,3,5}^{\infty} a_n \cos \frac{n\pi x}{2L} \qquad (B8)$$

$$u_F = \sum_{n=1,3,5}^{\infty} b_n \sin \frac{n\pi x}{2L} \qquad (B9)$$

$$u_L = \sum_{n=1,3,5}^{\infty} c_n \sin \frac{n\pi x}{2L} \qquad (B10)$$

Substituting the expressions (B8), (B9), and (B10) into equations (B5) and (B6) and then using expression (B7), where the variation is with respect to the a's, b's, c's, and C independently, results in the following equations (where $i = 1, 3, 5, \ldots$):

$$\left[\left(\frac{i\pi}{2}\right)^2 - k_S{}^2 k_B{}^2\right] a_i + \frac{L}{a}\frac{i\pi}{2} b_i - 2k_S{}^2 k_B{}^2 \frac{2}{i\pi}(-1)^{\frac{i-1}{2}} C = 0 \quad (B11)$$

$$\frac{a}{L}\frac{A_T}{A_F}\frac{i\pi}{2} a_i + \left[k_S{}^2\left(\frac{i\pi}{2}\right)^2 + k_S{}^2(KL)^2 \frac{A_L}{A_T} + \frac{A_T}{A_F}\right] b_i - k_S{}^2(KL)^2 \frac{A_L}{A_T} c_i = 0 \quad (B12)$$

$$\frac{A_F}{A_T}(KL)^2 b_i - \left[\left(\frac{i\pi}{2}\right)^2 + \frac{A_F}{A_T}(KL)^2\right] c_i = 0 \quad (B13)$$

$$k_B{}^2\left[C + \sum_{n=1,3,5}^{\infty} \frac{2}{n\pi} a_n(-1)^{\frac{n-1}{2}}\right] = 0 \quad (B14)$$

These equations are written in terms of $k_S$, the coefficient of shear rigidity, $K$, the shear-lag parameter, and $k_B$, the frequency coefficient; these terms are defined as follows:

$$k_S = \frac{1}{L}\sqrt{\frac{EI}{GA_S}} \quad (B15)$$

$$K = \sqrt{\frac{Gt_C}{Eb_S}\frac{A_T}{A_F A_L}} \quad (B16)$$

$$k_B = \omega\sqrt{\frac{\mu L^4}{EI}} \quad (B17)$$

where

$$A_S = 4at_W \quad (B18)$$

$$I = 4a^2 A_T \quad (B19)$$

$$A_T = A_F + A_L \quad (B20)$$

By solving equations (B11), (B12), and (B13) for $a_i$ and substituting the result into equation (B14), the following frequency equation, which must be satisfied by the frequency coefficient $k_B$, is obtained:

$$k_B^2\left[1 + 2k_B^2 k_S^2 \sum_{n=1,3,5}^{\infty}\left(\frac{2}{n\pi}\right)^2 \frac{1}{P_n - \frac{1}{N_n}\left(\frac{n\pi}{2}\right)^2}\right] = 0 \qquad (B21)$$

where

$$N_n = 1 + \frac{k_S^2\left[\left(\frac{n\pi}{2}\right)^2 + (KL)^2\right]\left(\frac{n\pi}{2}\right)^2}{\frac{A_T}{A_F}\left(\frac{n\pi}{2}\right)^2 + (KL)^2} \qquad (B22)$$

$$P_n = \left(\frac{n\pi}{2}\right)^2 - k_B^2 k_S^2 \qquad (B23)$$

The rate of convergence of the series of equation (B21) is increased by subtracting the expression $2k_B^4 k_S^2 \sum_{n=1,3,5}^{\infty} \frac{1}{\left(\frac{n\pi}{2}\right)^2 P_n}$ and adding the equivalent closed-form expression $k_B^2\left(\frac{\tan k_B k_S}{k_B k_S} - 1\right)$. The resulting equation is

$$k_B^2\left[\tan k_B k_S + 2k_B^3 k_S^3 \sum_{n=1,3,5}^{\infty}\frac{1}{P_n^2 N_n - P_n\left(\frac{n\pi}{2}\right)^2}\right] = 0 \qquad (B24)$$

The series in equation (B21) converges as $1/n^4$ while the series in equation (B24) converges as $1/n^6$.

For the case where $b/a \longrightarrow \infty$, equation (B21) reduces to the closed form

$$k_B^2\left(\alpha_1 \tanh k_B\alpha_1 + \beta_1 \tan k_B\beta_1\right) = 0 \qquad (B25)$$

where

$$\alpha_1 = \sqrt{-\frac{1}{2}\frac{Eb_Sb}{GL^2} + \frac{1}{2}\sqrt{\left(\frac{Eb_Sb}{GL^2}\right)^2 + \frac{4}{k_B^2}}} \qquad (B26)$$

and

$$\beta_1 = \sqrt{\frac{1}{2}\frac{Eb_Sb}{GL^2} + \frac{1}{2}\sqrt{\left(\frac{Eb_Sb}{GL^2}\right)^2 + \frac{4}{k_B^2}}} \qquad (B27)$$

For the case where $b_S = 0$, equation (B21) reduces to the closed form

$$k_B^2\left(\alpha_2\ \tanh\ k_B\alpha_2 + \beta_2\ \tan\ k_B\beta_2\right) = 0 \qquad (B28)$$

where

$$\alpha_2 = \sqrt{-\frac{1}{2}k_S^2 + \frac{1}{2}\sqrt{k_S^4 + \frac{4}{k_B^2}}} \qquad (B29)$$

$$\beta_2 = \sqrt{\frac{1}{2}k_S^2 + \frac{1}{2}\sqrt{k_S^4 + \frac{4}{k_B^2}}} \qquad (B30)$$

This frequency equation is identically the equation obtained when the frequency equation for symmetrically vibrating free-free beams of reference 4 is modified by neglecting rotary inertia, that is, when the only secondary effect considered is transverse shear deformation.

Mode shapes of the structure may be obtained by solving equations (B11), (B12), and (B13) for $a_i$, $b_i$, and $c_i$ and then substituting the results into expressions (B8), (B9), and (B10); the value of $C$ may be arbitrarily chosen.

Extension to the antisymmetrical modes and to cantilevered beams may be accomplished by methods similar to those shown in reference 1.

## APPENDIX C

## EXACT FREQUENCY SOLUTION FOR A DUAL-THICKNESS RECTANGULAR TUBE

The exact solution of reference 1 can be extended to take into account the effects of having different normal-stress- and shear-carrying thicknesses  $t'$  and  $t$  by modifying the expression for the maximum strain energy as follows:

$$U = \frac{1}{2} \int_0^L \oint E \left[ \frac{\partial u(x,s)}{\partial x} \right]^2 t'\, ds\, dx +$$

$$\frac{1}{2} \int_0^L \oint G \left[ \frac{\partial u(x,s)}{\partial s} + \frac{dw}{dx} \sin \theta \right]^2 t\, ds\, dx \qquad (C1)$$

The expression for maximum kinetic energy is unchanged if longitudinal inertia is neglected and is

$$T = \frac{1}{2} \int_0^L \mu \omega^2 w^2\, dx \qquad (C2)$$

By means of the procedure described in reference 1, the following frequency equation can be obtained for a symmetrically vibrating, free-free "dual-thickness" rectangular tube:

$$k_B^2 \left[ 1 + k_B^2 \sum_{n=1,3,5}^{\infty} \left( \frac{2}{n\pi} \right)^2 \frac{1}{N_n'} \right] = 0 \qquad (C3)$$

where

$$N_n' = \frac{n^2 \pi}{8 k_S^2} \left\{ \pi - \frac{K'}{4 k_S^2 n} \frac{p}{a} \left[ \frac{\sinh \frac{n\pi}{2} \frac{k_S}{K'} \left( \frac{8a}{p} - 1 \right)}{\cosh \frac{n\pi}{2} \frac{k_S}{K'}} + \tanh \frac{n\pi}{2} \frac{k_S}{K'} \right] \right\} - \frac{1}{2} k_B^2$$

$$(C4)$$

and

$$K' = \frac{4}{p}\sqrt{\frac{I}{A_S'}} \qquad\qquad (C5)$$

$$k_S = \frac{1}{L}\sqrt{\frac{EI}{GA_S}} \qquad\qquad (C6)$$

$$A_S' = 4at' \qquad\qquad (C7)$$

$$A_S = 4at \qquad\qquad (C8)$$

It should be noted that, with the exception of the slight change in parameters, equations (C3) and (C4) are the same as equations (41) and (A18) in reference 1 if, of course, the effects of longitudinal inertia are neglected.

## REFERENCES

1. Budiansky, Bernard, and Kruszewski, Edwin T.:  Transverse Vibrations
   of Hollow Thin-Walled Cylindrical Beams.  NACA TN 2682, 1952.

2. Anderson, Roger A., and Houbolt, John C.:  Effect of Shear Lag on
   Bending Vibration of Box Beams.  NACA TN 1583, 1948.

3. Kuhn, Paul, and Peterson, James P.:  Shear Lag in Axially Loaded
   Panels.  NACA TN 1728, 1948.

4. Kruszewski, Edwin T.:  Effect of Transverse Shear and Rotary Inertia
   on the Natural Frequency of a Uniform Beam.  NACA TN 1909, 1949.

TABLE 1

A COMPARISON OF ERRORS FOR OPTIMUM VALUES OF $b_S/b_C$

AND FOR A VALUE OF $b_S/b_C$ of 0.5

| Plan-form aspect ratio $L/b = 6.0$ | | | |
|---|---|---|---|
| Cross-sectional aspect ratio, $b/a$ | Optimum value of $b_S/b_C$ | Maximum percentage error for - | |
| | | Optimum value of $b_S/b_C$ | $b_S/b_C = 0.5$ |
| 1.0 | 0.65 | 0.5 | 1 |
| *3.6 | .56 | 1 | 2 |
| ∞ | .54 | 2 | 2.5 |
| Cross-sectional aspect ratio $b/a = 3.6$ | | | |
| Plan-form aspect ratio, $L/b$ | Optimum value of $b_S/b_C$ | Maximum percentage error for - | |
| | | Optimum value of $b_S/b_C$ | $b_S/b_C = 0.5$ |
| 2.0 | 0.44 | 2.5 | 3.5 |
| *6.0 | .56 | 1 | 2 |
| 12.0 | .61 | .5 | 1.5 |
| Cross-sectional aspect ratio $b/a = 3.6$; plan-form aspect ratio $L/b = 6.0$ | | | |
| Thickness ratio, $t'/t$ | Optimum value of $b_S/b_C$ | Maximum percentage error for - | |
| | | Optimum value of $b_S/b_C$ | $b_S/b_C = 0.5$ |
| *1.0 | 0.56 | 1 | 2 |
| 2.0 | .48 | 1.5 | 2 |

*This case is repeated for ease of comparison.
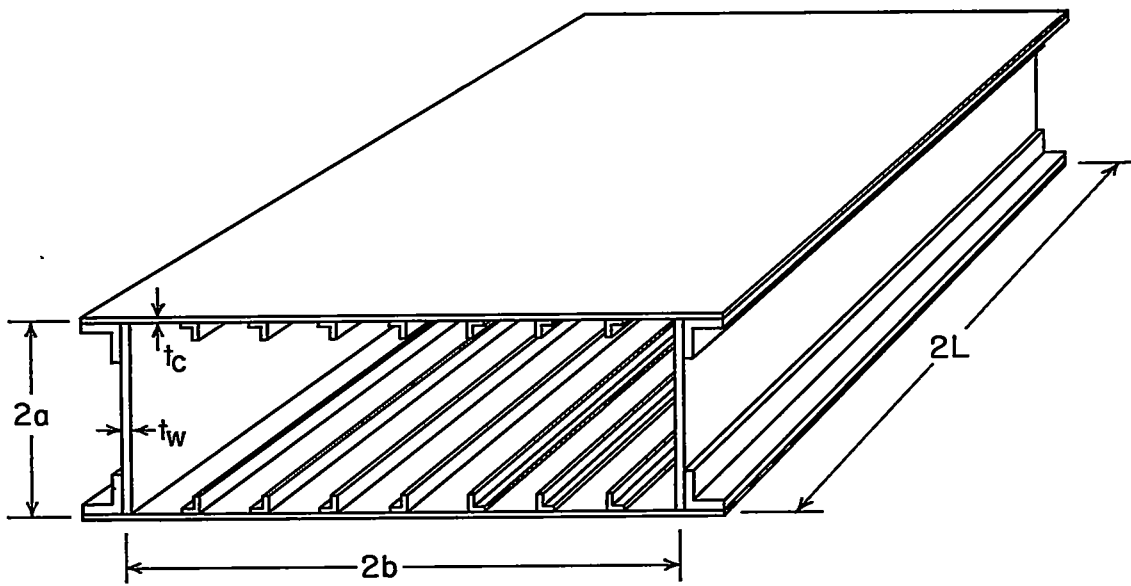
(a) Typical box beam.
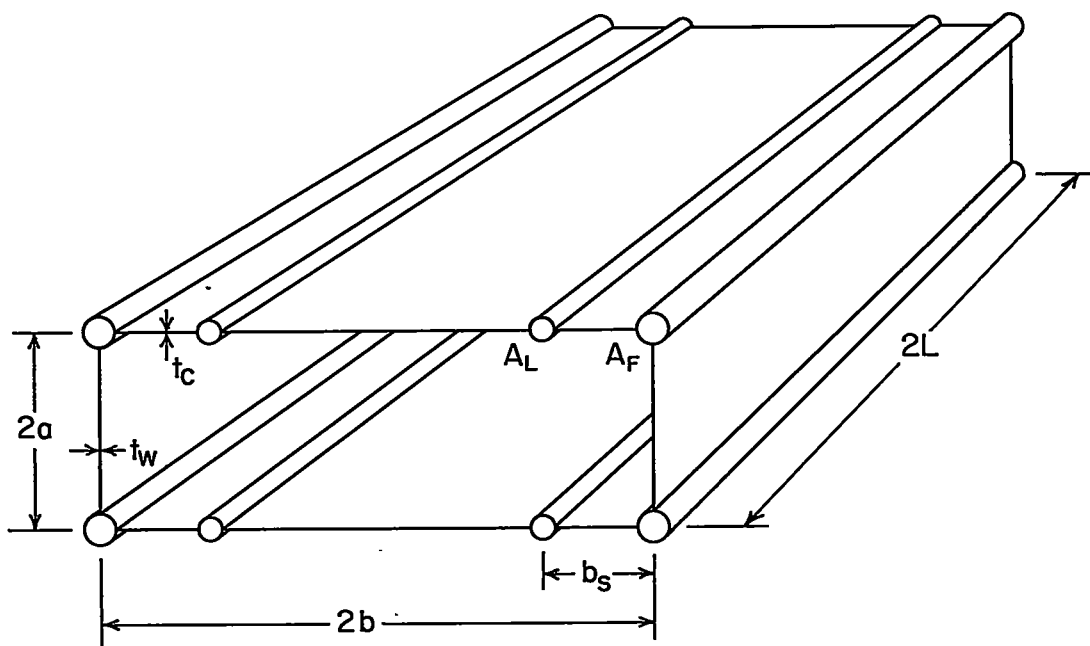


(b) Substitute-stringer idealization.

Figure I.–   Typical  box  beam   and its substitute-stringer idealization.
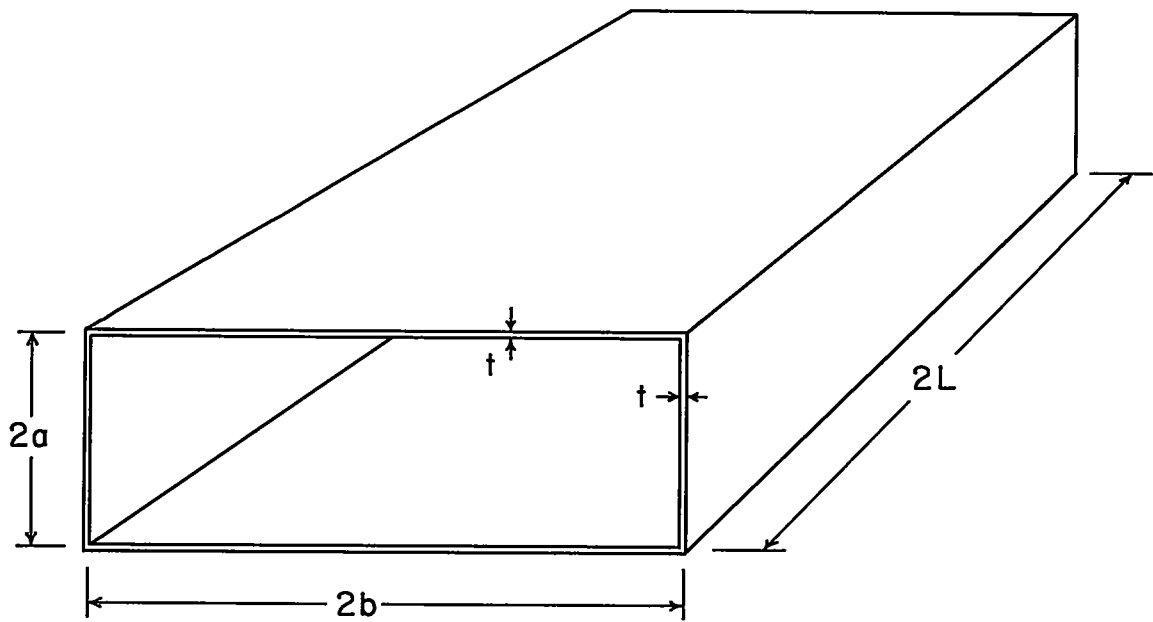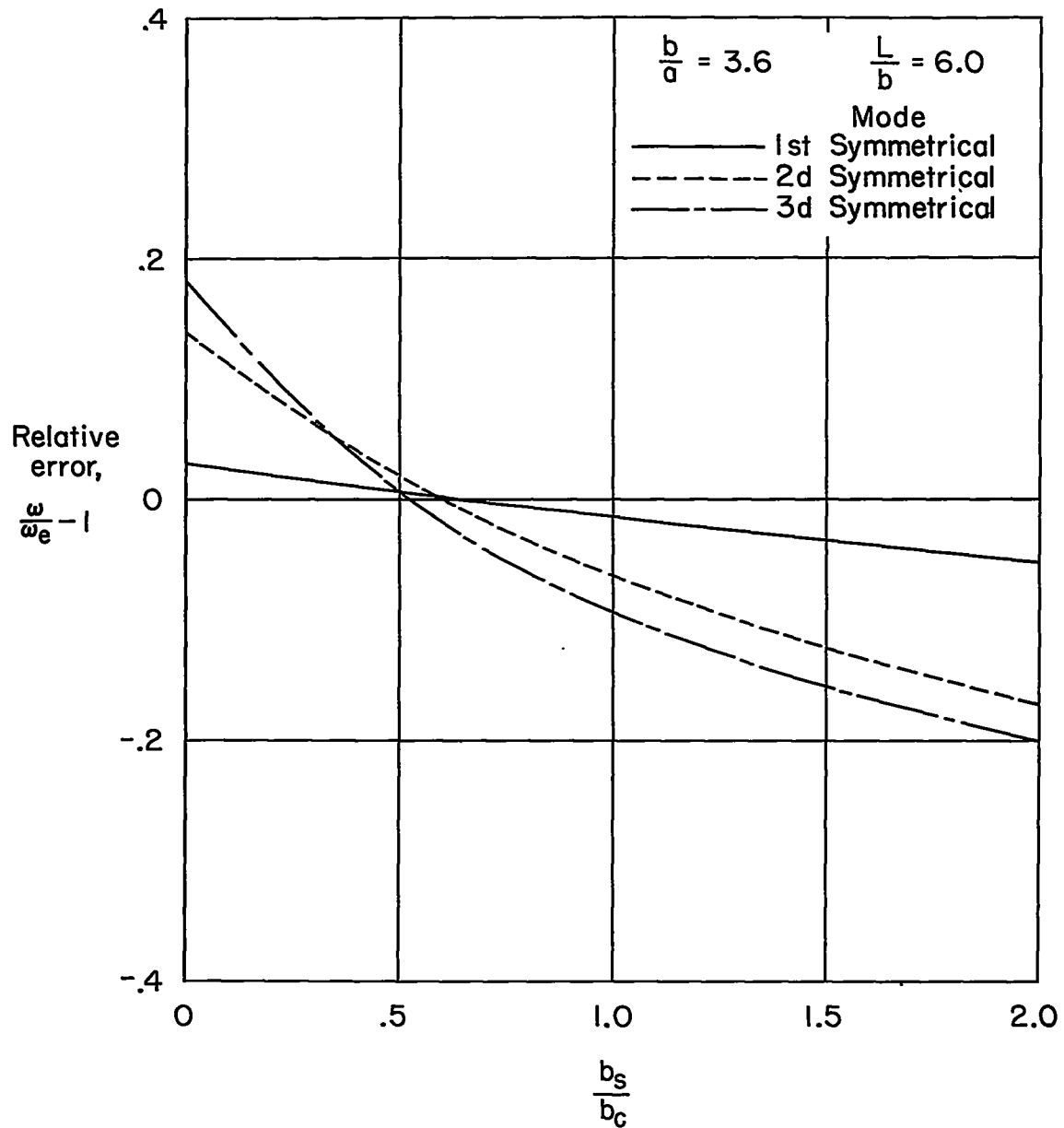
Figure 2.- Thin-walled rectangular tube.

Figure 3.- Effect of stringer location on the accuracy of the substitute-stringer approach for a box beam of uniform wall thickness.
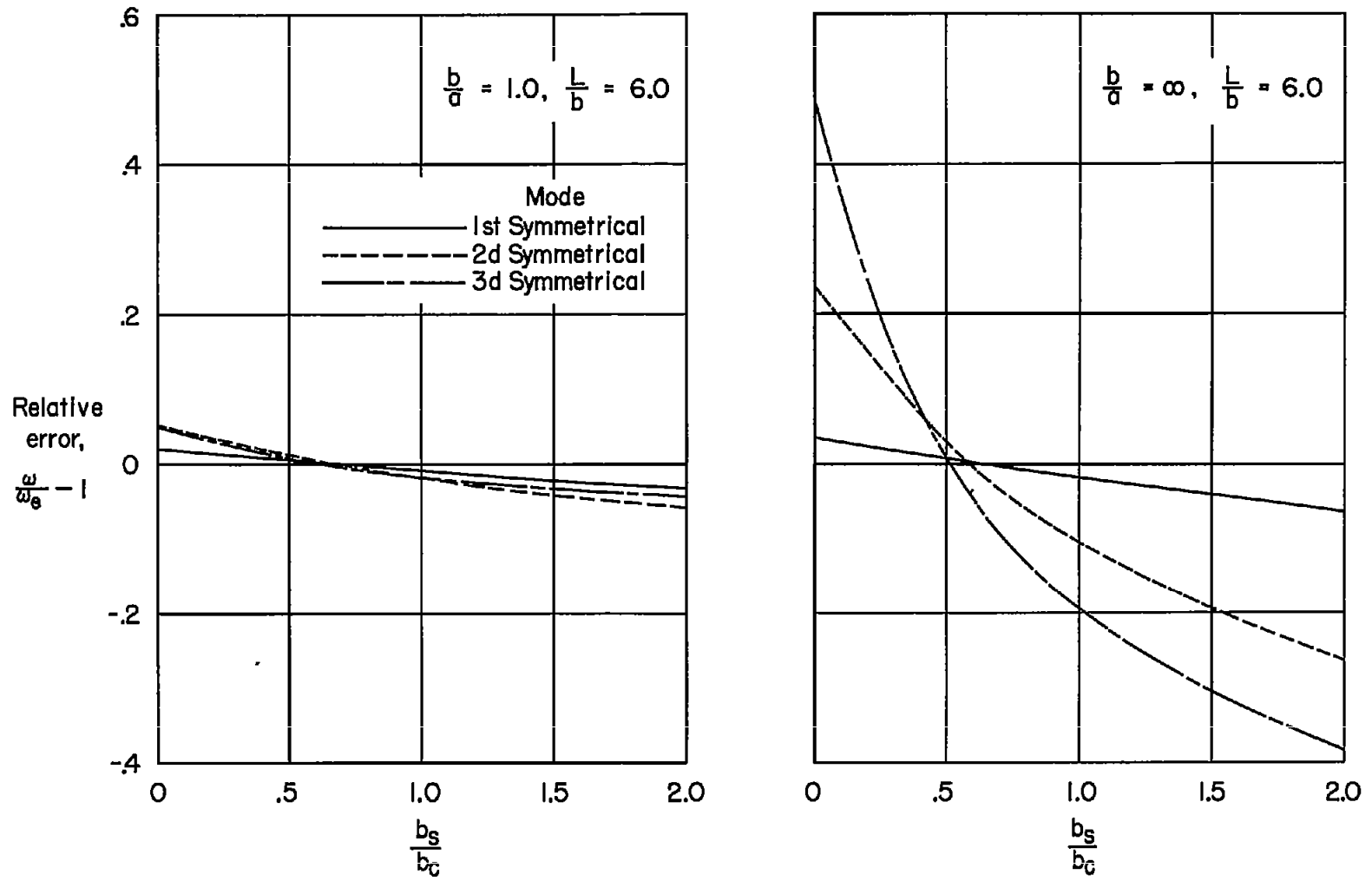
Figure 4.- Effect of stringer location on the accuracy of the substitute-stringer approach for box beams with extreme cross-sectional aspect ratios.
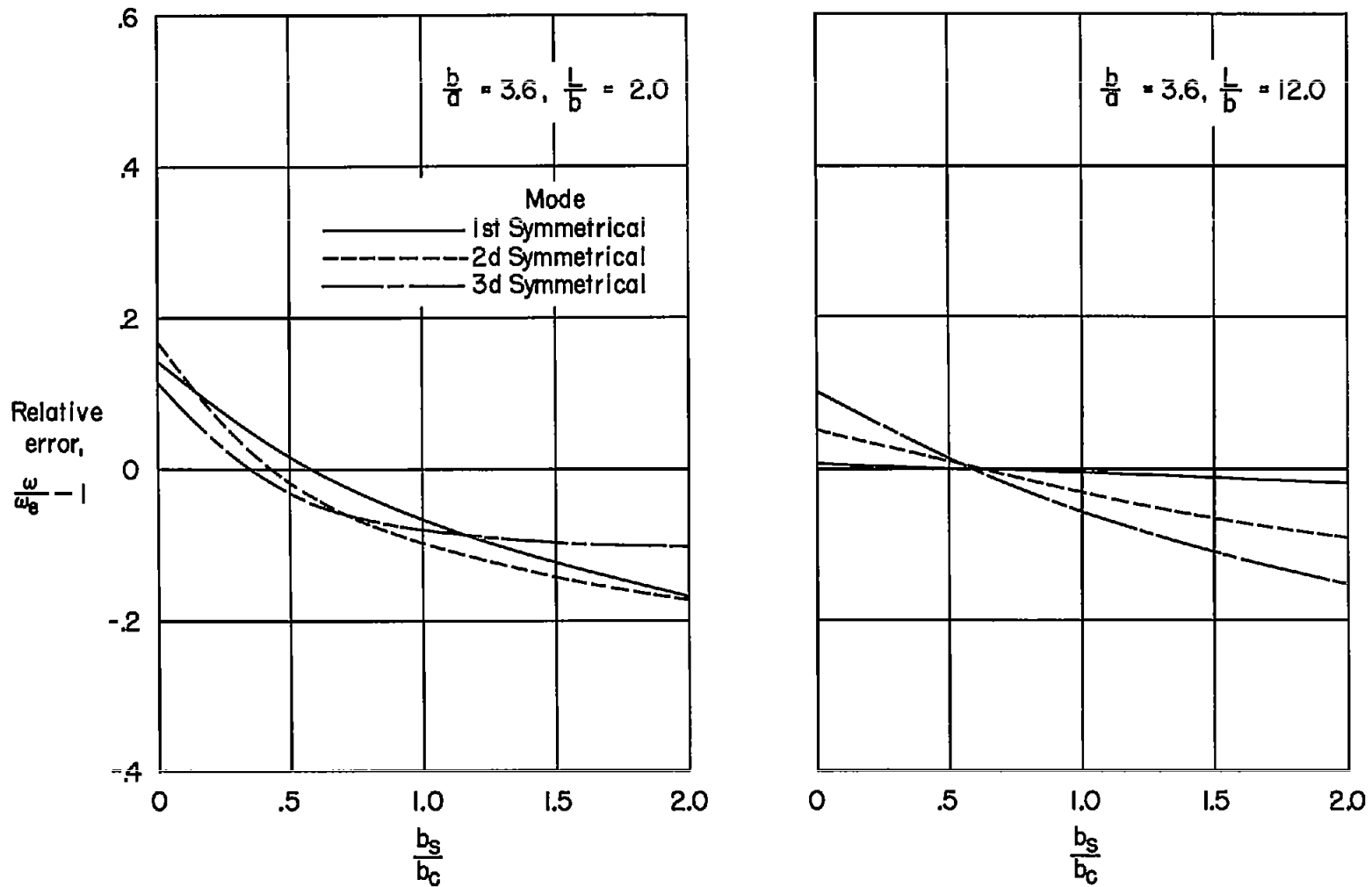
Figure 5.- Effect of stringer location on the accuracy of the substitute-stringer approach for box beams with extreme plan-form aspect ratios.
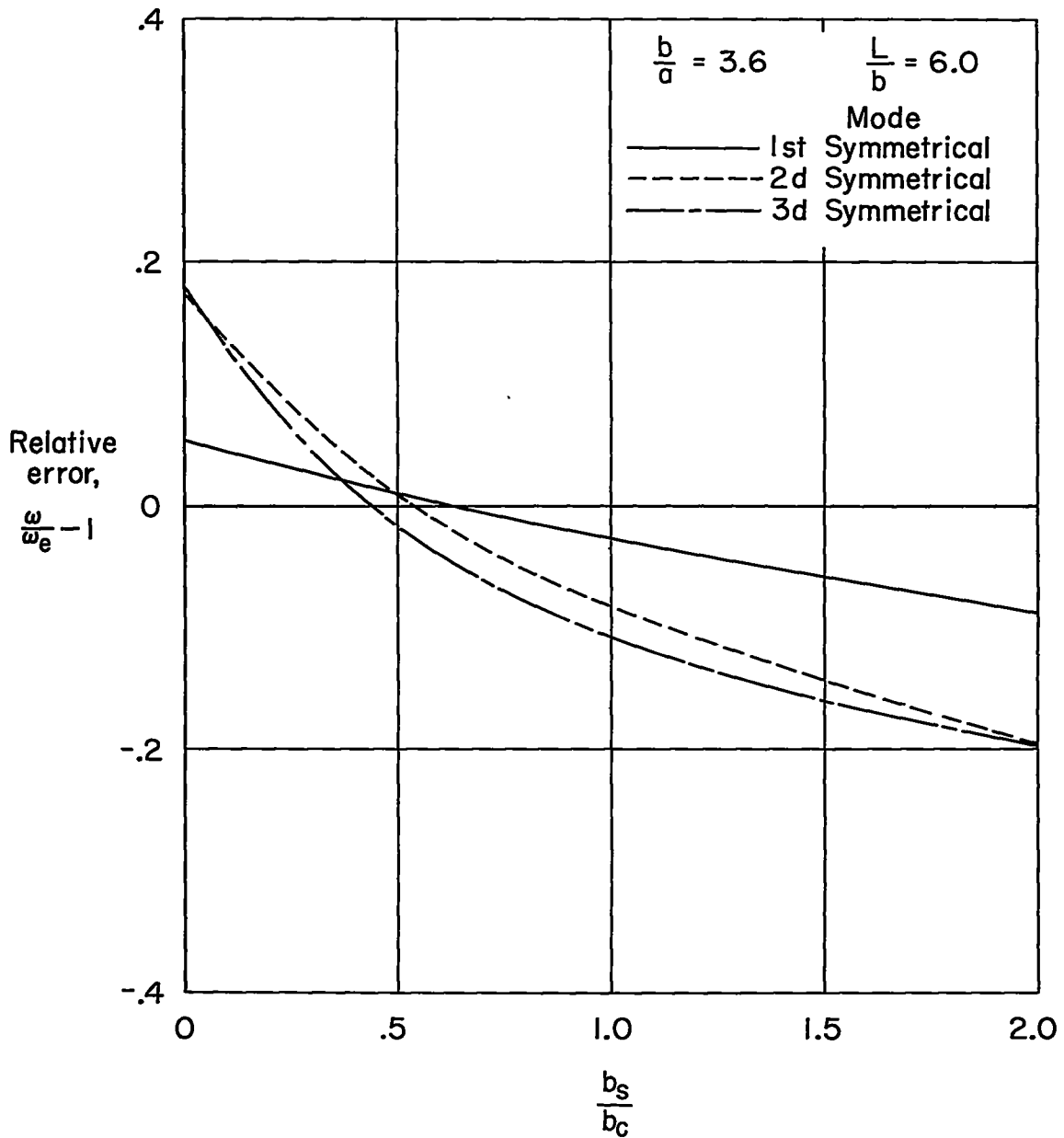
Figure 6. - Effect of stringer location on the accuracy of the substitute-stringer approach for a dual-thickness box beam $\left(\frac{t'}{t}=2\right)$.